Proc. Natl. Acad. Sci. USA
Vol. 89, pp. 9297–9301, October 1992
Genetics

Point mutations in the tyrosine aminotransferase gene in tyrosinemia type II

(Richner–Hanhart syndrome/inborn error of metabolism/complex allele/splice mutation)

ERNST NATT*†, KAICHI KIDA‡, MICHELE ODIEVRE§, MAJA DI ROCCO¶, AND GERD SCHERER*||

*Institute of Human Genetics, University of Freiburg, Breisacher Str. 33, D-7800 Freiburg, Federal Republic of Germany; ‡Department of Pediatrics, Ehime University School of Medicine, Ehime 791-02, Japan; §Hopital A. Béclère, Service de Pediatrie, F-92141 Clamart, France; and ¶2^A Divisione Medicina Pediatria, Istituto Gaslini, I-16148 Genova, Italy

Communicated by Susumu Ohno, June 5, 1992

ABSTRACT **Tyrosinemia type II (Richner–Hanhart syndrome, RHS) is a disease of autosomal recessive inheritance characterized by keratitis, palmoplantar hyperkeratosis, mental retardation, and elevated blood tyrosine levels. The disease results from deficiency in hepatic tyrosine aminotransferase (TAT; L-tyrosine:2-oxoglutarate aminotransferase, EC 2.6.1.5), a 454-amino acid protein encoded by a gene with 12 exons. To identify the causative mutations in five *TAT* alleles cloned from three RHS patients, chimeric genes constructed from normal and mutant *TAT* alleles were tested in directing TAT activity in a transient expression assay. DNA sequence analysis of the regions identified as nonfunctional revealed six different point mutations. Three RHS alleles have nonsense mutations at codons 57, 223, and 417, respectively. One "complex" RHS allele carries a GT → GG splice donor mutation in intron 8 together with a Gly → Val substitution at amino acid 362. A new splice acceptor site in intron 2 of the fifth RHS allele leads to a shift in reading frame.**

Tyrosinemia type II, also known as Richner–Hanhart syndrome (RHS), is an inborn error of metabolism due to a block in the transamination reaction converting tyrosine to *p*-hydroxyphenylpyruvate, a step catalyzed by the hepatic cytosolic enzyme tyrosine aminotransferase (TAT; L-tyrosine:2-oxoglutarate aminotransferase, EC 2.6.1.5). RHS patients suffer from keratitis, palmar and plantar hyperkeratosis, and sometimes mental retardation, accompanied by highly elevated serum and urine levels of tyrosine and its metabolites. The condition improves rapidly on a tyrosine- and phenylalanine-restricted diet (for reviews see refs. 1 and 2).

TAT has been extensively studied in rat and mouse, revealing a complex pattern of regulation. Enzyme activity is virtually absent in fetal rat liver and becomes detectable just after birth (3). The *TAT* gene is under hormonal control by glucocorticoids and cAMP, which increase the basal transcription rate 5- to 10-fold (4, 5), acting via different response elements in the 5′ flanking region of the gene (6, 7). Furthermore, the rodent *TAT* genes are subject to two trans-acting regulators. Basal expression and hormone inducibility of the *Tat* gene on mouse chromosome 8 are controlled by a positive trans-acting factor, alf, encoded on mouse chromosome 7 (8). Conversely, the tissue-specific extinguisher locus *Tse-1* on mouse chromosome 11 encodes a product that represses *Tat* gene transcription in nonliver cells (9).

Little is known about the regulation of the human *TAT* gene. As in rodents, hepatic TAT activity reaches significant levels shortly after birth, although some activity is present in the fetus (10). Induction of human TAT by glucocorticoids and cAMP has been demonstrated in fetal liver organ cultures (11). Moreover, there is evidence for a Tse-1-like factor on human chromosome 17 (9).

The human *TAT* gene extends over 10.9 kilobases (kb) containing 12 exons, and its 3.0-kb mRNA codes for a 454-amino acid protein of 50.4 kDa (12). We previously described an RHS patient with an inherited and a *de novo* deletion of the *TAT* locus at chromosome 16q22 (13). We now report the molecular defects underlying the RHS phenotypes in three nondeletion tyrosinemia type II patients.

MATERIALS AND METHODS

Patients. RHS patients studied are TI from Japan (14), MT from France (15), and MB from Italy. Age at onset of eye and skin lesions was 3–4 years for MB, and about 10 and 15 years, respectively, for her tyrosinemic brother. Untreated plasma tyrosine levels were 1.21 mM for MB and 1.05 mM for her brother, diagnosed at the age of 23 years and 27 years, respectively. Psychomotor development was normal in both sibs.

DNA Cloning and Sequence Analysis. To isolate 13-kb *Spe* I fragments harboring the complete 10.9-kb human *TAT* gene (12), 100 μg of genomic DNA was digested with *Spe* I and fractionated by electrophoresis in 0.7% agarose, and fragments of 11–15 kb were isolated and cloned into the *Xba* I site of EMBL12 (16) by standard techniques (17). Positive recombinants were identified by plaque hybridization of the resulting libraries (2.5×10^5 to 1.1×10^6 recombinants) with *TAT* cDNA clone phcTAT2-16 (12). Complete inserts were transferred as *Sal* I fragments into pSPSV, a derivative of pSP65 with the 180-base-pair (bp) *Hin*dIII–*Pvu* II fragment adjacent to the polylinker segment replaced by a 323-bp *Hin*dIII–*Pvu* II fragment from pSV2cat (18) carrying the simian virus 40 enhancer region. Subfragments cloned into M13 were sequenced (19) using Sequenase (United States Biochemical).

Construction of Chimeric *TAT* Genes. For constructs BII-1 and BII-2 (Fig. 1), 5.0-kb *Bgl* II fragments were removed from each pSPSV clone to generate deletion clones (designated pSPSVdB), purified by cloning into pUC vectors, and reinserted into the deletion clones in the appropriate combinations. Constructs X-1 and X-2 were obtained accordingly, making use of an *Xba* I site in the polylinker. For constructs H-1 and BII-1/H, the 5.0-kb *Bgl* II fragments of the normal TAT allele and of allele RHS2B were cloned into a pUC derivative lacking a *Hin*dIII site. These subclones were used to exchange the 2.7-kb *Hin*dIII fragment in the manner described, and the resulting chimeric *Bgl* II fragments were

The publication costs of this article were defrayed in part by page charge payment. This article must therefore be hereby marked "*advertisement*" in accordance with 18 U.S.C. §1734 solely to indicate this fact.

Abbreviations: TAT, tyrosine aminotransferase; RHS, Richner–Hanhart syndrome.

†Present address: Institut National Polytechnique, ENSAT, 145 Avenue de Muret, F-31076 Toulouse, France.
||To whom reprint requests should be addressed.

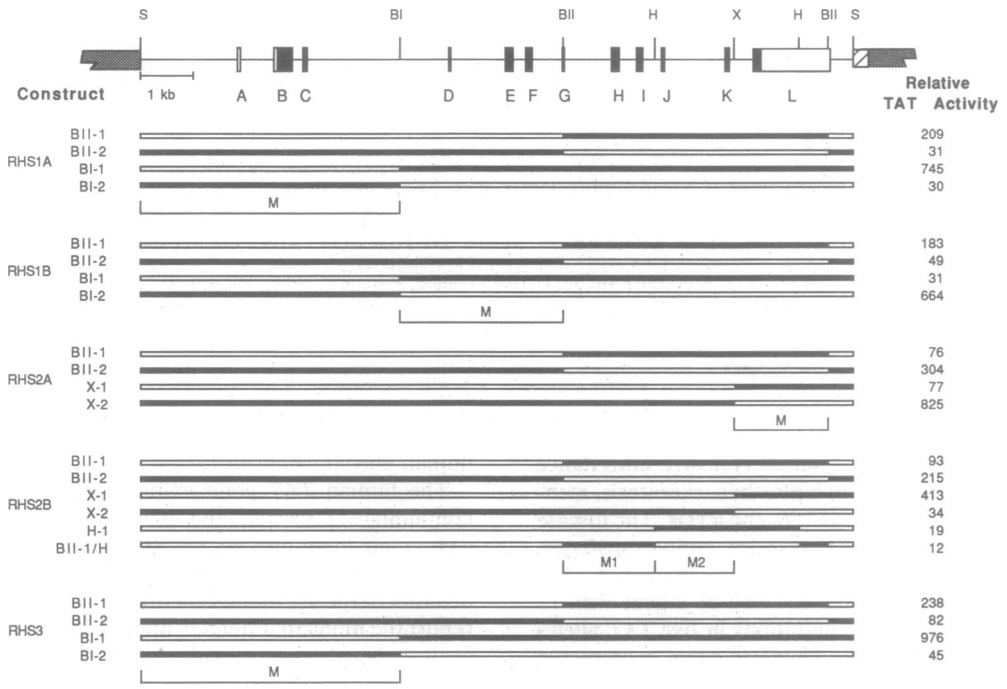

FIG. 1. Functional transfection assays of chimeric *TAT* genes identify regions harboring inactivating mutations. Chimeric *TAT* genes were constructed by combining fragments from mutant alleles (black segments) with those from the wild-type allele (open segments) in plasmid vector pSP65 carrying the simian virus 40 enhancer. Plasmid constructs were cotransfected with RSVlacZ plasmid as internal standard into mouse Ltk$^-$ fibroblasts. Enzyme activity of cell extracts prepared after transient expression for 45–53 hr is given as relative TAT activity (TAT specific activity × 1000/β-galactosidase specific activity). Exons A–L of the *TAT* gene (12) are indicated at the top, with coding sequences indicated by black boxes, and 5′ and 3′ untranslated regions by white boxes. Vector segments are shaded, and the simian virus 40 enhancer fragment is hatched. Relevant restriction sites: BI, *Bgl* I; BII, *Bgl* II; H, *Hin*dIII; S, *Sal* I; X, *Xba* I. Regions containing inactivating mutations as defined by relative TAT activities below 100 are indicated by M. Note that allele RHS2B carries two mutations, M1 and M2.

reinserted into the wild-type pSPSVdB clone. Generation of constructs BI-1 and BI-2 was more complex (20).

Transient Transfection Assay. One day before transfection, 2×10^6 mouse Ltk$^-$ cells (thymidine kinase-deficient fibroblast line) were seeded in 10-cm dishes and grown in Dulbecco's modified Eagle's medium (DMEM) containing 10% fetal bovine serum. Plasmid DNA [9 μg of test plasmid plus 1 μg of RSVlacZ plasmid (gift of W. Ankenbauer, German Cancer Research Center, Heidelberg), a derivative of pCH110 (36) containing the Rous sarcoma virus long terminal repeat promoter/enhancer] was then added in 3 ml of transfection solution consisting of DMEM, 20 mM Hepes (pH 7.4), 0.1 mM chloroquine diphosphate, and 0.2 mg of DEAE-dextran per ml. Transfection solution was removed after 5 hr, and cells were incubated for 40–48 hr in normal medium. Cells from one dish were harvested in 250 μl of TAT buffer (21) and sonified, and extracts were cleared by centrifugation at 10,000 × *g*. TAT assays (21) were performed with 60 μl of extract, after a preincubation step at 75°C for 2 min to inactivate nonspecific transaminases. The β-galactosidase assay (22) was carried out with 40 μl of extract.

Nuclease S1 Mapping. A 600-bp genomic fragment of RHS1A, extending from a *Hin*dIII site in intron 2 to an *Ava* I site 75 bp into exon C, was cloned, after fill-in of the restriction sites, into *Sma* I-cut M13mp19, regenerating an *Ava* I site close to the universal sequencing primer. Dideoxy-sequencing products obtained from this clone, designated 19HA3, were cut with *Ava* I, resulting in a sequence ladder directly aligning with the nuclease S1-resistant products. To generate the nuclease S1 probe fragment, clone 19HA3 was cut with *Ava* I, 5′ end-labeled, and cut with *Dde* I, and a 135-bp *Dde* I–*Ava* I fragment labeled at the *Ava* I site in exon C was isolated. This probe fragment (0.04 pmol) was mixed in 10 μl of hybridization solution with total RNA isolated from mouse Ltk$^-$ cells 21 hr after transfection with mutant allele RHS1A (40 μg of RNA) or normal *TAT* allele (20 μg of RNA) or from untransfected cells (20 μg of RNA). Hybridization and nuclease S1 digestion were essentially as described (23), except that RNA·DNA hybrids were allowed to form at 52°C for 8 hr, then at 50°C for 4 hr, and finally at 48°C for 4 hr.

RESULTS

Cloning and Differentiation of *TAT* Alleles. When this analysis was started, the DNA sequence of the exons and their flanking intron borders in the human *TAT* gene had not yet been determined (12), precluding a PCR-based approach. We therefore cloned normal and mutant *TAT* alleles on 13-kb restriction fragments containing the complete 10.9-kb TAT gene into plasmid vectors. The normal *TAT* allele is derived from clone λhTAT1 (12), whereas the mutant *TAT* alleles are from three RHS patients (TI, MT, and MB). Eight independent clones each were isolated from TI and MT, and six from MB.

Results of allele differentiation by restriction pattern analysis are presented in Table 1. Alleles RHS1A and RHS1B, represented by five and three clones, respectively, differ only in their *Hph* I pattern. Alleles RHS2A and RHS2B, also represented by five and three clones, respectively, can be differentiated by eight enzymes. No differences were found among the six independent clones from patient MB. The differences observed with *Bam*HI and *Hae* III are true restriction fragment length polymorphisms (24, 25) and have allowed us to identify, by pedigree analysis, RHS2A as the maternal allele and RHS2B as the paternal allele (24).

Functional Transfection Assay of Chimeric *TAT* Genes. To narrow down the region(s) harboring the mutant site(s) in each RHS allele, a series of chimeric *TAT* clones was constructed by exchanging restriction fragments between normal and mutant *TAT* alleles (Fig. 1). For every mutant

Table 1. Comparison of restriction enzyme cleavage patterns of cloned RHS alleles with those of the normal *TAT* allele

Enzyme	Patient TI		Patient MT		Patient MB,
	RHS1A (5 clones)	RHS1B (3 clones)	RHS2A (5 clones)	RHS2B (3 clones)	RHS3 (6 clones)
Alu I	+	+	+	−	+
*Bam*HI	+	+	−	+	+
Bst NI	+	+	+	−	+
Dde I	+	+	+	−	+
Hae III	+	+	−	+	+
*Hin*fI	+	+	+	−	+
Hph I	+	−	+	−	+
Rsa I	+	+	+	−	+

Plasmid pUC18 subclones containing *TAT* alleles on 13-kb genomic *Spe* I (*Sal* I) fragments, cloned in the same orientation, were digested with 10 frequently cutting restriction enzymes and with *Bam*HI. Resulting fragments from normal and mutant *TAT* alleles were separated in 2% agarose gels side by side. +/−, identical to/different from normal *TAT* allele. No differences were observed with *Hha* I, *Hpa* II, and *Sau*3A1.

allele, a 5.0-kb *Bgl* II fragment was exchanged, allowing a differentiation of the 5′ and 3′ halves of the gene. Further exchanges took place at the *Bgl* I site between exons C and D (for RHS1A, RHS1B, and RHS3) and at the *Xba* I site between exons K and L (for RHS2A and RHS2B). Finally, for RHS2B only, a 2.7-kb *Hin*dIII fragment from the 3′ end of the gene was exchanged. Resulting plasmids were tested for directing TAT activity in mouse Ltk$^-$ fibroblasts after cotransfection with plasmid RSVlacZ, using β-galactosidase activity as internal standard to compensate for variable transfection efficiencies. Constructs giving relative TAT activities below 100 were scored as carrying inactivating mutations, which could be narrowed down to the regions marked by brackets (M) in Fig. 1. Interestingly, RHS2B carries two mutations, M1 and M2, each being sufficient for complete inactivation.

Identification of the *TAT* Mutations by DNA Sequence Analysis. All exons and exon/intron boundaries, as well as the first 200 bp of the 5′ flanking region, within the relevant regions thus identified were subjected to DNA sequence analysis on appropriate M13 subclones. The autoradiographs in Fig. 2 display the mutations identified, which are summarized in Fig. 3.

Each mutation turned out to be a single base substitution, except for the deletion of a CT dinucleotide at positions −8 and −7 in the promoter region of RHS3 (data not shown). Three mutations generate stop codons in exons F, L, and B of alleles RHS1B (Fig. 2*B*), RHS2A (Fig. 2*C*), and RHS3 (Fig. 2*F*), respectively. One mutation leads to an exchange from Gly to Val in codon 362 within exon J of RHS2B (Fig. 2*E*; region M2 in Fig. 1). This mutation, a G → T transversion, occurs within the sequence CCT-G(G/T)A-CTC (codons 361–363), thus destroying restriction sites for *Bst*NI (CCTGG) and *Hin*fI (GACTC) and generating a new *Rsa* I site (GTAC) (compare Table 1).

Finally, two mutations occur at splice junctions. The second inactivating mutation of RHS2B (Fig. 2*D*; region M1 in Fig. 1) changes the conserved GT splice donor sequence at the exon H/intron 8 boundary to GG. The second splice mutation, an A → G transition in intron 2 of RHS1A (Fig. 2*A*), creates a new splice acceptor site (see below). Due to the new splice occurring four nucleotides 5′ to the normal splice position, a new reading frame results, terminating at codon 91/92 in exon C.

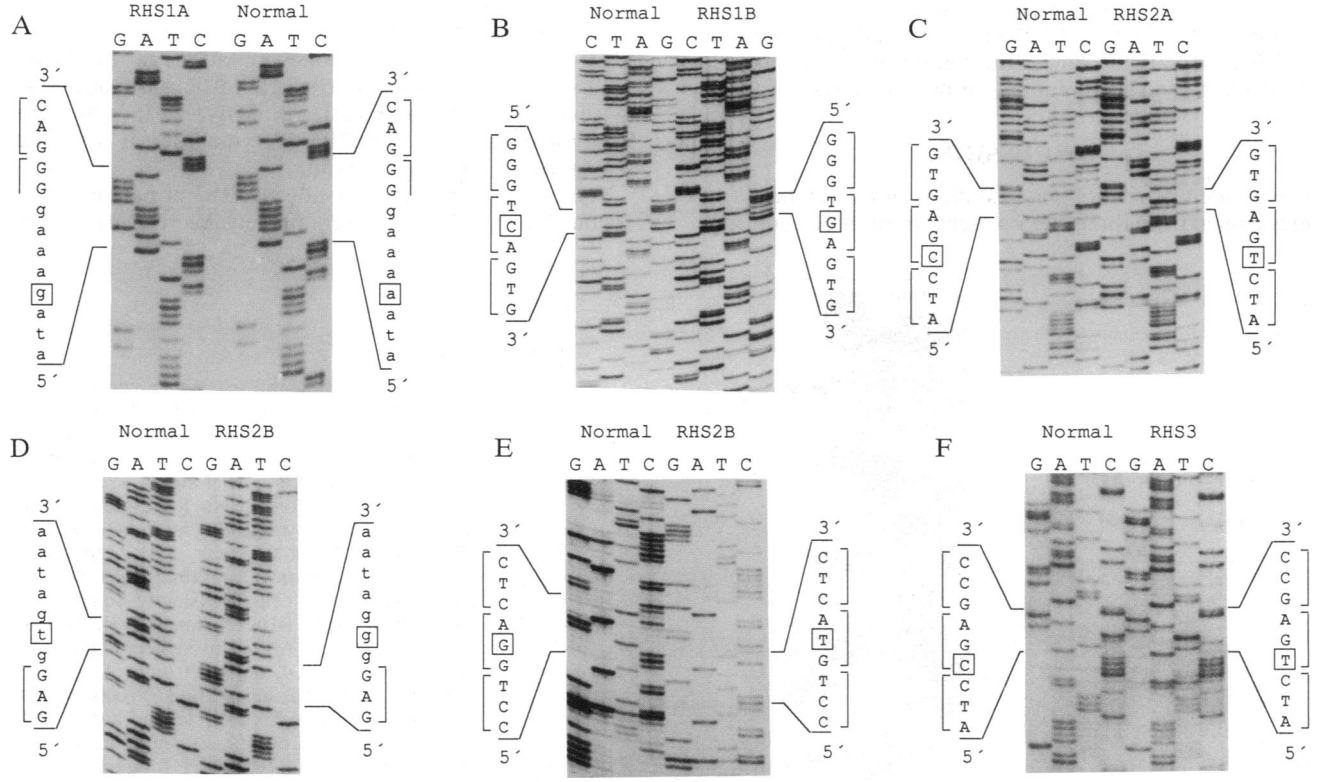

FIG. 2. RHS alleles from patients TI, MT, and MB carry different point mutations. Autoradiographs are from 6% polyacrylamide sequencing gels, with ^{35}S-labeled sequencing products obtained from M13 subclones of mutant and normal *TAT* alleles run side by side. Relevant segments shown are from intron 2/exon C (*A*), exon F (*B*), exon L (*C*), exon H/intron 8 (*D*), exon J (*E*), and exon B (*F*). The sequence read from the autoradiographs is of RNA-like polarity except for *B*, where labeling of sequence lanes has been transposed. The slight shift in the sequencing ladder of RHS2B in *E* is due to a deletion in the M13 polylinker that occurred during subcloning. Exon sequences are in uppercase, intron sequences in lowercase. The reading frame is indicated by brackets, and nucleotides affected by mutations are boxed. The consequences of the observed mutations are summarized in Fig. 3.

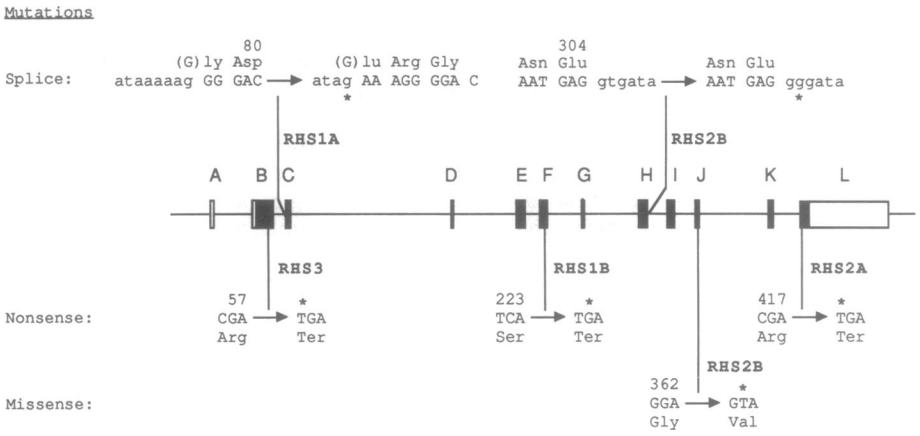

FIG. 3. Summary of point mutations and of their consequences in the five RHS alleles analyzed. The positions of the six point mutations identified (Fig. 2) are given with respect to the exon/intron map of the *TAT* gene. Exon sequences are in uppercase, intron sequences in lowercase. Relevant codons are numbered, and mutant nucleotides are marked by an asterisk. The RHS1A mutation generates a novel splice acceptor site that is efficiently used (Fig. 4). Ter, termination.

Nuclease S1 Analysis of the RHS1A Splice Acceptor Mutation in Intron 2. A 135-bp *Dde* I–*Ava* I fragment, 5′-end-labeled in the coding strand of the *TAT* gene at an *Ava* I site in exon C, was used as probe in nuclease S1 analysis. Hybridization to total RNA from Ltk⁻ cells transiently transfected with the normal or RHS1A mutant *TAT* allele yields protected DNA fragments of larger size under less stringent nuclease S1 conditions (Fig. 4, lanes 1, 2, 4, and 5), while more stringent conditions lead to prominent fragments of the expected size for the mutant (lane 3) and normal (lane 6) *TAT* allele that are exactly four nucleotides apart. (Note that because the G ribonucleotide residue at the 3′ end of exon B can base pair with the C deoxyribonucleotide residue at the 3′ end of intron 2 of both the normal and mutant *TAT* allele, the S1 analysis can at best identify the nucleotide preceding the start of the normal and mutant exon C, as indicated at left in Fig. 4.) Because virtually no wild-type signal appears in Fig. 4, lane 3, the mutant splice acceptor site of RHS1A is used preferentially, if not exclusively.

DISCUSSION

We have identified six point mutations in five mutant *TAT* alleles cloned from three RHS patients from three countries. All mutations are different, scattered over the whole 12-exon human *TAT* gene. Two stop codon mutations, in exons B and L, result from C → T transitions in CGA (Arg) codons (Fig. 2 *C* and *F* and Fig. 3), the CG dinucleotide being a well-known mutational hotspot (26). In accordance with the absence of TAT activity in liver biopsy samples of patients TI and MT (14, 15), their RHS alleles carry strong inactivating mutations: a splice mutation in one allele (RHS1A for TI, RHS2B for MT) and a nonsense mutation in the second allele (RHS1B for TI, RHS2A for MT) (Figs. 2 and 3).

We have demonstrated experimentally for allele RHS1A that the new splice acceptor site in intron 2 is used in high preference over the wild-type splice site (Fig. 4), resulting in a shift of reading frame and premature termination of translation at codons 91/92 in the mutant TAT mRNA. For allele RHS2B, the molecular consequences of the GT → GG splice donor mutation in intron 8 have not been investigated. Identical GT → GG splice donor mutations in the β-globin gene and in the factor IX gene lead to β^0-thalassemia (27) and to severe hemophilia B (28), respectively. It is therefore highly likely that the RHS2B splice mutation is a similarly strong loss-of-function mutation.

The nonsense mutation in allele RHS3 of patient MB, at codon 57 in exon B, is also a completely inactivating mutation

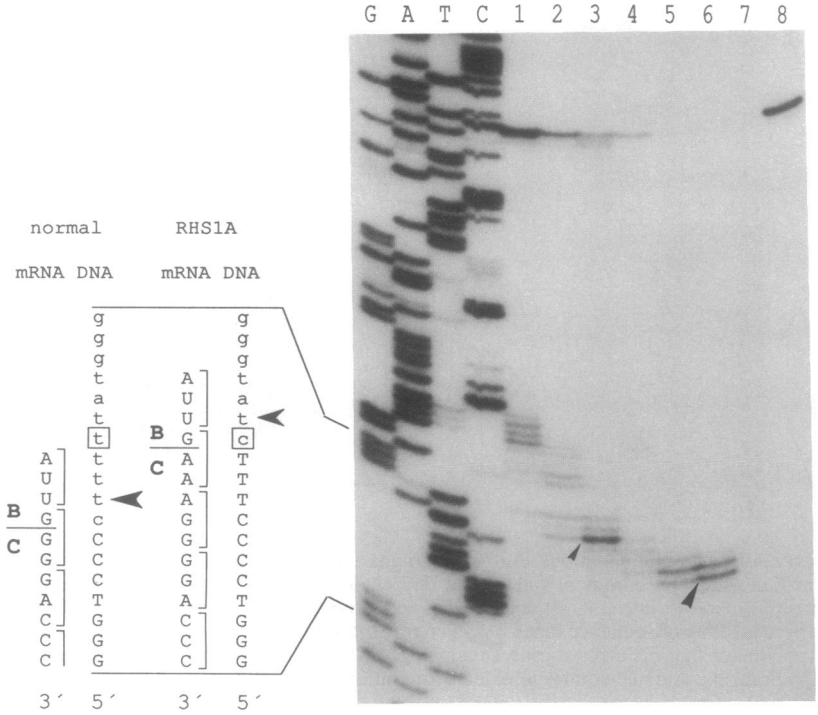

FIG. 4. The new intron 2 splice acceptor site of allele RHS1A is efficiently used. Lanes G, A, T, and C show the dideoxy sequencing ladder obtained from a 600-bp *Hin*dIII–*Ava* I fragment of RHS1A, starting at an *Ava* I site in exon C and extending into intron 2. Nuclease S1-resistant products obtained by digesting hybrids between a 135-bp *Dde* I–*Ava* I fragment, 5′-end-labeled at the *Ava* I site in exon C, and total RNA isolated from mouse Ltk⁻ cells transiently transfected with mutant allele RHS1A (lanes 1–3), normal *TAT* allele (lanes 4–6), or untransfected (lane 7), are shown. Lanes 1, 4, and 7, 200 units of nuclease S1 per ml, 1 hr, 25°C; lanes 2 and 5, 1000 units of nuclease S1 per ml, 1 hr, 25°C; lanes 3 and 6, 1000 units of nuclease S1 per ml, 30 min, 37°C; lane 8, untreated 135-bp *Dde* I–*Ava* I fragment. Most prominent nuclease S1-resistant fragments of mutant and normal *TAT* alleles are marked by the small and large arrowheads in lanes 3 and 6, respectively. The corresponding positions in the sequences shown at left are marked accordingly. The reading frame in the mRNA sequence is indicated by brackets; the nucleotide affected by the mutation is boxed.

(Figs. 2*F* and 3). The second mutation observed in this allele, the deletion of a CT dinucleotide at positions −8 and −7 in the *TAT* promoter region (data not shown), which changes the distance between the TATA box and the start site of transcription from 27 to 25 bp, probably has no severe consequences. The corresponding distance within the herpes simplex thymidine kinase promoter region could be changed over a much wider range, for example, before a reduction in transcription rate was observed (29).

It is possible that patient MB is homozygous for the RHS3 allele. First, all six independent clones analyzed gave the same restriction patterns (Table 1), and all six had the same CT dinucleotide deletion in the *TAT* promoter region (data not shown). Second, restriction fragment length polymorphism analysis for *TAT* and the flanking loci haptoglobin and chymotrypsinogen B on chromosome 16q (30), for which the parents are informative, shows that MB and her tyrosinemic brother are both homozygous at all three loci (unpublished data). Although consanguinity is not reported in this family, the parents could be related, both coming from a small village of about 1500 inhabitants in Lombardy.

A surprising observation is the presence of two inactivating mutations in allele RHS2B (Fig. 2 *D* and *E* and Fig. 3). While the nature of the intron 8 splice donor mutation clearly indicates a severe functional defect as discussed, the Gly → Val exchange at residue 362 encoded in exon J seems less dramatic. However, the functional test provided by the transfection assay demonstrates that the region designated M2 in Fig. 1 between the *Hin*dIII and *Xba* I sites flanking exons J and K, respectively, indeed carries a strong loss-of-function mutation. While the existence of a new splice signal in the 1.1-kb intron between exons J and K has not been ruled out, the substitution at position 362 of valine for glycine, a residue conserved in rat TAT (12), is not a trivial polymorphism, as demonstrated by absence of the *Rsa* I site diagnostic for this substitution in PCR fragments from the exon J region of 50 unrelated individuals (data not shown). Presence of the more bulky side chain of valine in place of the hydrogen atom contributed by glycine could possibly interfere with proper folding or dimerization of the TAT protein, whose enzymatically active form is a homodimer (31). For example, a Gly → Val exchange at a site of close contact between α-helices B and E in β-globin of hemoglobin Savannah leads to destabilization and complete inactivation of the protein (32). Alleles like RHS3 containing more than one mutation, designated "complex" alleles, although rare, have been observed in other autosomal recessive disorders (33, 34).

The RHS2A nonsense mutation at codon 417 indicates that the carboxyl-terminal 38 amino acid residues are essential for TAT enzyme function (Figs. 2*C* and 3). This contrasts with the amino terminus, where the first 64 amino acid residues can be removed from rat TAT without any loss of enzyme activity (35). Correspondingly, the amino-terminal 64 residues in the human and rat TAT protein differ at 18 positions, whereas the carboxyl-terminal 38 residues are identical (12). Analysis of further cases of RHS, in addition to providing insight into the molecular heterogeneity of tyrosinemia type II, may identify other residues critical for TAT enzyme activity.

We thank W. Ankenbauer for plasmid RSVlacZ, R. J. Jäger and T. F. Wienker for comments on the manuscript, and C. Sehabiague and E. Kunstmann for typing. This work was supported by a grant from the Deutsche Forschungsgemeinschaft (Sche 194/4).

1. Buist, N. R. M., Kennaway, N. G. & Fellmann, J. H. (1985) in *Inherited Diseases of Amino Acid Metabolism*, eds. Bickel, H. & Wachtel, U. (Thieme, Stuttgart), pp. 203–235.
2. Goldsmith, L. A. & Laberge, C. (1989) in *The Metabolic Basis of Inherited Disease*, eds. Scriver, C. R., Beaudet, A. L., Sly, W. S. & Valle, U. (McGraw-Hill, New York), pp. 547–562.
3. Greengard, O. (1970) in *Biochemical Actions of Hormones*, ed. Litwack, G. (Academic, New York), Vol. 1, pp. 53–87.
4. Hashimoto, S., Schmid, W. & Schütz, G. (1984) *Proc. Natl. Acad. Sci. USA* **81**, 6637–6641.
5. Schmid, E., Schmid, W., Jantzen, M., Mayer, D., Jastorff, B. & Schütz, G. (1987) *Eur. J. Biochem.* **165**, 499–506.
6. Jantzen, H.-M., Strähle, U., Gloss, B., Stewart, F., Schmid, W., Boshart, M., Miksicek, R. & Schütz, G. (1987) *Cell* **49**, 29–38.
7. Boshart, M., Weih, F., Schmidt, A., Fournier, R. E. K. & Schütz, G. (1990) *Cell* **61**, 905–916.
8. Ruppert, S., Boshart, M., Bosch, F. X., Schmid, W., Fournier, R. E. K. & Schütz, G. (1990) *Cell* **61**, 895–904.
9. Killary, A. M. & Fournier, R. E. K. (1984) *Cell* **38**, 523–534.
10. Andersson, S. M., Räihä, N. C. R. & Ohisalo, J. J. (1980) *J. Dev. Physiol.* **2**, 17–27.
11. Andersson, S. M. (1981) *Early Hum. Dev.* **6**, 165–169.
12. Rettenmeier, R., Natt, E., Zentgraf, H. & Scherer, G. (1990) *Nucleic Acids Res.* **18**, 3853–3861.
13. Natt, E., Westphal, E.-M., Toth-Fejel, S. E., Magenis, R. E., Buist, N. R. M., Rettenmeier, R. & Scherer, G. (1987) *Hum. Genet.* **77**, 352–358.
14. Kida, K., Takahashi, M., Fujisawa, Y., Matsuda, H., Machino, H. & Miki, Y. (1982) *J. Inherited Metab. Dis.* **5**, 229–230.
15. Lemonnier, F., Charpentier, C., Odievre, M., Larregue, M. & Lemonnier, A. (1979) *J. Pediatr.* **94**, 931–932.
16. Natt, E. & Scherer, G. (1986) *Nucleic Acids Res.* **14**, 7128.
17. Sambrook, J., Fritsch, E. F. & Maniatis, T. (1989) *Molecular Cloning: A Laboratory Manual* (Cold Spring Harbor Lab., Cold Spring Harbor, NY).
18. Gorman, C. M., Moffat, L. F. & Howard, B. H. (1982) *Mol. Cell. Biol.* **2**, 1044–1051.
19. Sanger, F., Nicklen, S. & Coulson, A. R. (1977) *Proc. Natl. Acad. Sci. USA* **74**, 5463–5467.
20. Natt, E. (1988) Ph.D. thesis (Albert-Ludwigs-Universität, Freiburg, Federal Republic of Germany).
21. Diamondstone, T. I. (1966) *Anal. Biochem.* **16**, 395–401.
22. Platt, T., Müller-Hill, B. & Miller, J. H. (1972) in *Experiments in Molecular Genetics*, ed. Miller, J. H. (Cold Spring Harbor Lab., Cold Spring Harbor, NY), pp. 352–355.
23. Schmid, W., Scherer, G., Danesch, U., Zentgraf, H., Matthias, P., Strange, C. M., Röwekamp, W. & Schütz, G. (1982) *EMBO J.* **1**, 1287–1293.
24. Westphal, E.-M., Natt, E., Grimm, T., Odievre, M. & Scherer, G. (1988) *Hum. Genet.* **79**, 260–264.
25. Wullich, B., Natt, E., Wienker, T. F. & Scherer, G. (1989) *Nucleic Acids Res.* **17**, 3331.
26. Green, P. M., Montandon, A. J., Bentley, D. R., Ljung, R., Nilsson, I. M. & Gianelli, F. (1990) *Nucleic Acids Res.* **18**, 3227–3231.
27. Chibani, J., Vidaud, M., Duquesnoy, P., Bergé-Lefranc, J. L., Pirastu, M., Ellouze, F., Rosa, J. & Goossens, M. (1988) *Hum. Genet.* **78**, 190–192.
28. Brownlee, G. G. (1988) *Recent Adv. Haematol.* **5**, 251–265.
29. McKnight, S. L., Gavis, E. R., Kingsbury, R. & Axel, R. (1981) *Cell* **25**, 385–398.
30. Westphal, E.-M., Burmeister, M., Wienker, T. F., Lehrach, H., Bender, K. & Scherer, G. (1987) *Genomics* **1**, 313–319.
31. Andersson, S. M. & Pispa, J. P. (1982) *Clin. Chim. Acta* **125**, 117–123.
32. Huisman, T. H. J., Brown, A. K., Efremov, G. D., Wilson, J. B., Reynolds, C. A., Uy, R. & Smith, L. L. (1971) *J. Clin. Invest.* **50**, 650–659.
33. Latham, T., Grabowski, G. A., Theophilus, B. D. M. & Smith, F. I. (1990) *Am. J. Hum. Genet.* **47**, 79–86.
34. Dörk, T., Wulbrand, U., Richter, T., Neumann, T., Wolfes, H., Wulf, B., Maass, G. & Tümmler, B. (1991) *Hum. Genet.* **87**, 441–446.
35. Hargrove, J. L., Scoble, H. A., Mathews, W. R., Baumstark, B. R. & Biemann, K. (1989) *J. Biol. Chem.* **264**, 45–53.
36. Hall, C., Jacob, E., Ringold, G. & Lee, F. (1983) *J. Mol. Appl. Genet.* **2**, 101–109.